Mech. Sci., 2, 139–146, 2011
www.mech-sci.net/2/139/2011/
doi:10.5194/ms-2-139-2011

Mechanical Sciences
Open Access

Design and principles of an innovative compliant fast tool servo for precision engineering

H. Li[1,*], R. Ibrahim[2], and K. Cheng[2]

[1]Department of Mechanical Design and Manufacturing, College of Engineering, China Agricultural University, Beijing 100083, China
[2]School of Engineering and Design, Brunel University, Uxbridge, UB8 3PH, UK
[*]currently at: Brunel University, Uxbridge, UB8 3PH, UK

Received: 7 March 2011 – Revised: 17 May 2011 – Accepted: 12 June 2011 – Published: 5 July 2011

Abstract. The paper presents an innovative design of fast tool servo (FTS) by combining compliant mechanism (CM) and precision engineering (PE) so as to meet the stringent requirements of a one degree of freedom (1DOF) compact FTS. The design requirements of the FTS include: (a) 1 nm resolution, (b) 10–20 μm of range, (c) first natural frequency of over 1400 Hz, (d) compatibility with holding different diamond cutting tools, and (e) without fatigue of the compliant mechanism. Then FEA is used to evaluate the static and dynamic performance of the FTS. The preliminary results show that both the static and dynamic performances are matched to the design objectives.

1 Introduction

The fast tool servo (FTS) plays important roles in precision turning of free-form surfaces with a diamond cutting tool. Some compliant mechanisms (CMs) have been applied in FTS because of their advantages such as no coulomb friction and no backlash (Howell, 2001). A piezoelectric actuator was often used in FTS because of its high resolution and wide bandwidth actuation. Many researchers studied the design and synthesis of the CMs (Li et al., 2010; Yu et al., 2010a, 2010b). But they seldom considered the actual application in precision engineering (PE). On the contrary some FTSs have been designed taking little account of the design principles of CMs (Cuttino et al., 1999; Gan et al., 2007; Huo and Cheng, 2008; Kim and Kim, 2003; Kim et al., 2004, 2009; Kouno, 1984; Noh et al., 2009; Spotts et al., 2004; Tian et al., 2009). Therefore, there is a need for a comprehensive and robust design method combining with CMs and PE to meet the stringent requirements of ultra precision machining.

Kouno (1984) designed a FTS CM that consists of two parallel diaphragms based on the parallel-spring concept but the stiffness of 70 N μm^{-1} of the CM consumed more energy and reduced the stroke. Cuttino (1999) used two annular flexures in his FTS but the design bandwidth is only 100 Hz. The CM with two sets of parallel circle notch flexure hinges was introduced by Gan et al. (2007), Huo and Cheng (2008), Kim and Kim (2003), Kim et al. (2004, 2009), Tian et al. (2009). Kim and Kim (2003) and Kim et al. (2004) designed a FTS giving a stroke and natural frequency of 7.5 μm and 100 Hz respectively. In order to increase the stroke of the FTS, a flexure mechanism amplifier was embedded on the CM and the stroke was increased to 432 μm but the stiffness decreased (Kim et al., 2009). Gan et al. (2007) pointed out that the dimensions of a CM were determined by the static stiffness along three directions and the stiffness of the CM of his FTS along the motion direction was 4.29 N μm^{-1}; the mass of the rigid part, the stroke and the natural frequency were 170 g, 4.6 μm and 69 Hz respectively. Tian et al. (2009) discovered the contact condition between the actuator and the rigid part of a CM was affected by a low stiffness; the maximum stress analyzed by using FEM was less than the yield limit of the material; the best stiffness was 13.1 N μm^{-1} by considering the contact condition and the stroke reduction; the mass of the rigid part could be reduced to a certain level to get the desired high dynamic frequency, 1122 Hz. Huo and Cheng (2008) put forward that the higher stiffness and first frequency of the CM reduce effectiveness of the piezoelectric actuator stoke. Both the theoretical calculation and FEA analysis of the CM were used to decide the dimension of the CM, the static stiffness and the first natural frequency. Therefore, the design method of the CM in FTS is not clear till now.

Correspondence to: K. Cheng
(kai.cheng@brunel.ac.uk)

Published by Copernicus Publications.

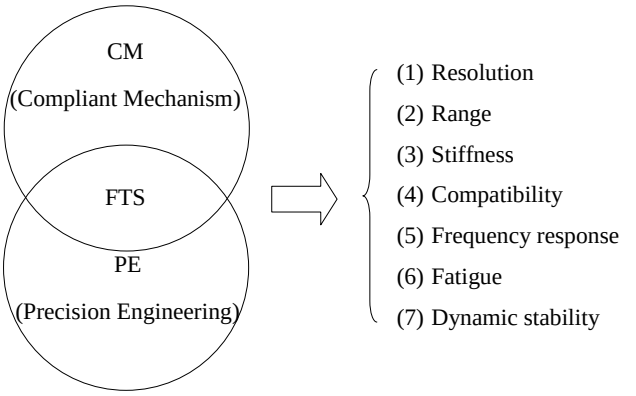

Figure 1. FTS is in the intersection of CM and PE and its design requirements are displayed.

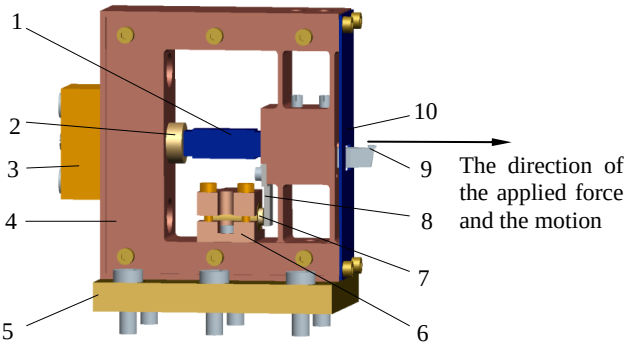

Figure 2. A schematic view of the FTS. The main parts concludes: (1) the piezoelectric actuator, (2) the preload screw, (3) the lock screw base, (4) the CM structure, (5) the base, (6) the sensor holder, (7) the sensor, (8) the sensor plate, (9) the cutting tool, and (10) the front cover.

This paper presents the design criteria and method of a CM to predetermine the dimensions of the CM in design stage. The CM in a FTS should satisfy the requirements of resolution, working range, higher first natural frequency, compatibility with holding various cutting tools and non-fatigue. Then an innovative design of a 1DOF linear FTS and its design principles are developed. FEA is used to evaluate the performance of the design in detail and preliminary results are obtained and discussed. Finally the conclusions are outlined.

2 Conceptual design and principles

A typical FTS consists of four major parts. They are a CM holding a cutting tool, a piezoelectric actuator, a displacement sensor and a control system. Therefore, the design of a FTS should be considered from both CM and PE. So the FTS is the intersection of CM and PE shown in Fig. 1. Based on the understanding of the FTS, there are seven critical parameters or issues that should be considered; they are resolution, range, stiffness, compatibility, frequency response, fatigue and dynamic stability.

An innovative design of FTS is designed to hold various diamond cutting tools and to perform turning operations as shown in Fig. 2. It consists of several parts: a CM structure, a piezoelectric actuator, a preload screw, a lock screw, a diamond cutting tool, a sensor, two covers on both sides, a front cover, a base, etc. The CM can be manufactured by wire-cut EDM to avoid machining errors.

Piezoelectric actuator has high resolution, high stiffness and high frequency response. Therefore a piezoelectric stacked actuator is used for larger stroke. Three different lengths of the stacked actuators which are 18 mm (PPA10M), 28 mm (PPA20M), and 48 mm (PPA40M) from Cedrat Technologies SA can be used in this research project. Different preload screws with corresponding length for each of the piezoelectric stacked actuators are used to house the actuators in the same CM. Spring steel material has been chosen in taking into account of greater Young's modulus.

The CM structure is symmetric and its rigid part can only move in one direction (axial direction), without movement along the other two directions (horizontal and vertical ones). The rigid part can hold various diamond cutting tools. The tool tip should move in the central line of the CM structure.

The working frequency of the FTS, f_{com}, is no more than the natural frequency, f_{com0}, of the CM. f_{com0} is decided by the mass of the rigid part of the CM structure, m_{s}, and the stiffness of the axial stiffness of the CM, K_{axial}, as expressed as

$$f_{\mathrm{com0}} = \frac{1}{2\pi}\sqrt{\frac{K_{\mathrm{axial}}}{m_{\mathrm{s}}}} \geq \frac{f_{\mathrm{com}}}{S_{\mathrm{f}}} \tag{1}$$

where S_{f} is the safety factor of the frequency response of the FTS.

The smaller the mass of the rigid part is, the higher the natural frequency becomes. However, the lower the axial stiffness is the lower the natural frequency turns out. While at the same time, a high stiffness will reduce the range of the FTS and consumes more energy. Therefore, two criteria should be considered when the natural frequency of the CM is decided. One criterion is the mass of the rigid part should be reduced to minimum. Another is the appropriate axial stiffness of the CM should be chosen.

The stiffness in other two directions, which are vertical stiffness, K_{vertical}, and horizontal stiffness, $K_{\mathrm{horizontal}}$, should be evaluated. They should be adequate in order that the tool tip will have very small displacement in the two directions.

Each beam bears maximum cyclic loading at both ends. The life cycle should be calculated to determine whether failure will occur.

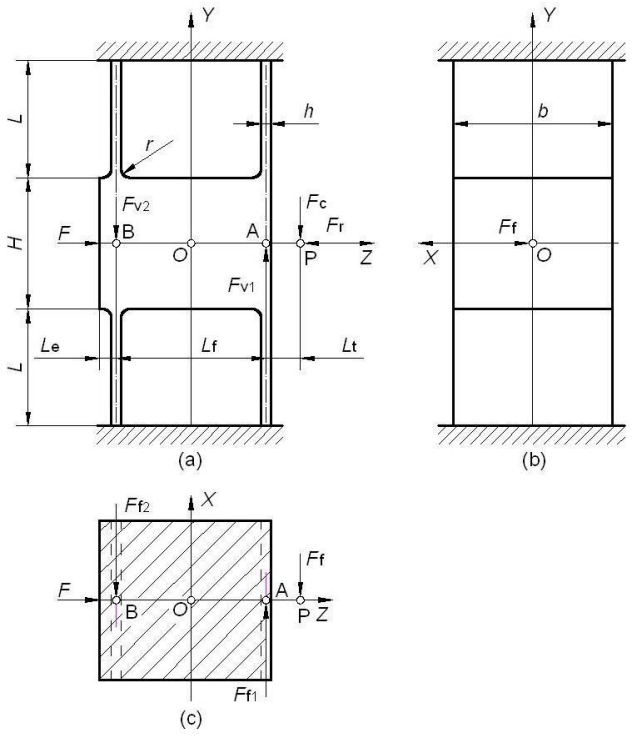

Figure 3. Three orthographic projections of the CM: **(a)** front view; **(b)** side view; **(c)** top view. The reference system (the origin O and the axes X, Y, and Z), the critical dimensions (L, H, b, h, L_e, L_f, L_t), the force components (the actuating force F, the cutting force F_c, the feed force F_f, and the thrust force F_r at the tool tip P; the reaction force F_{v1}, F_{f1} at the centre point A of the front set of beams, the reaction force F_{v2}, F_{f2} at the centre point B of the rear set of beams) are also displayed.

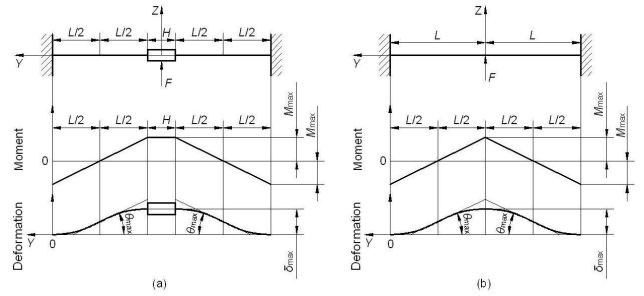

Figure 4. The moment, the deformation, and the rotated angle of the CM from **(a)** conceptual design and **(b)** simplified design. The maximum moment M_{max}, the maximum deformation δ_{max}, and the maximum rotated angle θ_{max} of the CM are also displayed.

3 Design analysis

3.1 The design of the CM

The CM consists of two sets of parallel beams; each set of beams is symmetric and fixed both ends with a rigid part and the base respectively. Figure 3 shows the three orthographic projections of the CM; the rigid part holds the tool.

The critical dimensions of the CM are shown in Table 1. The thickness (h), width (b) and length (L) of the beams play an important role in determining the stiffness of three directions. The beams also should be designed in fillet or radius to prevent the distribution of stress concentration. The width of the rigid part is the same as that of the beam.

A Cartesian coordinate has been defined. XOZ is in the horizontal symmetrical centre plane of the CM; XOY is in the vertical symmetrical plane of the CM. The tool tip, P, is located in Z-axis. The set of beams near the tool tip is called the front set of beams and the other one is the rear set of beams. The centric point of the front set of beams and the rear set of beams are A and B, respectively. When the tool is cutting a work piece, the force applied on the cutting tip is divided into three ones; they are cutting force, F_c, feed force, F_f and thrust force, F_r. The actuating force the actuator applies on the rigid part, F, is in the Z-axis direction.

The axial stiffness is much smaller than its vertical and horizontal stiffness. When an axial force is applied to the rigid part in Z-axis the rigid part will move; each beam will bear an axial shear and a tensile stress along its whole length, and bear a moment at both ends of each beam.

3.2 Stiffness

3.2.1 Axial stiffness

Each set of the beams of the CM, which we call the designed beam, can be regarded as a beam, which we call the simplified beam, with both fixed ends and a central load as shown in Fig. 4 because all the beams in both the designed beam and the simplified beam bear the same shear stress, tensile stress and moment.

The axial stiffness of the CM can be calculated according to the linear-elastic beam theory. For a beam with both fixed ends and a centre load, F_{axial}, the axial displacement, δ_{axial} at the centre of the beam, i.e., the axial displacement of the rigid part is expressed as (Howell, 2001; Noh et al., 2009)

$$\delta_{axial} = \frac{F_{axial}(2L)^3}{192EI} \tag{2}$$

where E is Young's Modulus and I is moment of inertia which is equal to $\frac{bh^3}{12}$.

So we can get

$$F_{axial} = 2Eb\left(\frac{h}{L}\right)^3 \delta_{axial} \tag{3}$$

Because there two sets of beams with both fixed ends and a centre load, the axial stiffness of the CM can be obtained

$$K_{axial} = 4Eb\left(\frac{h}{L}\right)^3 \tag{4}$$

Table 1. Critical dimensions of the CM.

Item	Definition	Value/mm
h	The thickness of the beam	1.7
b	The width of the beam	20
L	The length of the beam	20
H	The height of the rigid part	26
L_f	The distance between the two sets of beams in horizontal direction	18
L_e	The distance between the end of the rigid part and the rear set of beams in horizontal direction	6
L_t	The distance between the tip of the tool and the front set of beams in horizontal direction	13.85
r	The fillet of the CM	1.5

3.2.2 Horizontal stiffness

The horizontal stiffness of the two sets of beams with both fixed ends and a centre load are calculated respectively and they are equal. They are both calculated by using the same method used in calculating axial stiffness (see Eq. 3) except the moment of inertia is $\frac{b^3h}{12}$. The horizontal stiffness is expressed as below

$$K_{\text{horizontal}} = 2Eh\left(\frac{b}{L}\right)^3 \tag{5}$$

3.2.3 Vertical stiffness

The vertical stiffness of the two sets of beams with both fixed ends are also calculated respectively and they are equal as well as. Assumed the applied vertical force is F_{vertical}. The lengths of each beam in one set of beams are equal. The forces applied on each beam are equal but one beam is compressed and another is extended. Therefore, the forces applied on each beam are $F_{\text{vertical}}/2$. The equation is obtained as

$$E = \frac{\sigma}{\varepsilon} = \frac{F_{\text{vertical}}L}{2A_b\Delta L} \tag{6}$$

where ΔL is the length of extension, A_b is the sectional area of the beam and it is equal to bh.

Transforming Eq. (6), the vertical stiffness is expressed as

$$K_{\text{vertical}} = \frac{F_v}{\Delta L} = \frac{2EA_b}{L} = \frac{2Ebh}{L} \tag{7}$$

3.2.4 Comparison of the vertical and the horizontal stiffness

Because the FST is used for both face turning and outline turning the vertical stiffness should be equal to the horizontal stiffness. Letting Eq. (5) is equal to Eq. (7), we can obtain $b = L$ which means the length and the width of the beam are equal.

3.2.5 Comparison of the axial stiffness with the vertical/horizontal stiffness

Both the vertical stiffness and the horizontal stiffness should be high enough to ensure that the displacement of the tool tip remains very small in both the vertical and the horizontal directions. Comparing Eqs. (5) and (4), the ratio of vertical stiffness to axial stiffness is expressed as

$$\frac{K_{\text{horizontal}}}{K_{\text{axial}}} = \frac{1}{2}\left(\frac{b}{h}\right)^2 \tag{8}$$

3.2.6 Stiffness of the FTS

The actuator and the CM are in parallel connection. Therefore the stiffness of the FTS is equal to $K_{\text{FTS}} = K_{\text{act}} + K_{\text{axial}}$, where K_{act} is the stiffness of the actuator.

3.3 Natural frequency

The mass of the rigid part, which is approximately equal to a cube whose volume is the outline of the rigid part, is obtained as following equation

$$m_s = \rho(L_e + h + L_f)bH \tag{9}$$

where ρ is the density of the material, L_e the distance between the end of the rigid part and the rear set of beams in horizontal direction, L_f the distance between the two sets of beams in horizontal direction, H the height of the rigid part

The volume of the FTS should be compact. Therefore the length of the beam, L, or the width of the beam, b, are determined and the axial stiffness is obtained. According to Eq. (1), the natural frequency of the CM can be calculated.

3.4 Force and deformation analysis

3.4.1 Vertical force analysis and deformation analysis

The vertical forces applied to the two sets of beams, respectively, are

$$F_{v1} = \frac{L_t + L_f}{L_f}F_c \tag{10}$$

$$F_{v2} = \frac{L_t}{L_f} F_c \tag{11}$$

where L_t is the distance between the tip of the tool and the front set of beams in horizontal direction.

Correspond displacements according to $K_{horizontal}$ respectively are

$$\delta_{vi} = \frac{F_{vi}}{K_{vertical}} \quad (i = 1,2) \tag{12}$$

The reaction force and deformation in the front set of beams are bigger than those in the rear set of beams, respectively.

3.4.2 Horizontal force analysis and deformation analysis

The horizontal forces applied to the two sets of beams, respectively, are

$$F_{h1} = \frac{L_t + L_f}{L_f} F_f \tag{13}$$

$$F_{h2} = \frac{L_t}{L_f} F_f \tag{14}$$

Correspond displacements according to $K_{horizontal}$ respectively are

$$\delta_{hi} = \frac{F_{hi}}{K_{horizontal}} \quad (i = 1,2) \tag{15}$$

The reaction force and the deformation in the front set of beams are bigger than those in the rear of beams, respectively. The moment in the front set of beams bigger than that in the rear set of beams. The maximum moment locates at both ends of the beam and its value is

$$M_{h1} = \frac{F_{h1} L}{8} \tag{16}$$

3.4.3 Axial force and deformation analysis

The maximum moment occurs at both ends of each beam is shown as

$$M_{axial\,max} = \frac{\frac{F_{axial}}{2} 2L}{8} = \frac{F_{axial} L}{8} \tag{17}$$

where the maximum stress is calculated as below

$$\sigma_{axial\,max} = \frac{M_{axial\,max} c}{I} = \frac{\frac{F_{axial} L}{8} \frac{h}{2}}{\frac{bh^3}{12}} = \frac{3 F_{axial} L}{4bh2} \tag{18}$$

Substituting Eq. (3) into Eq. (18), the results is as following

$$\sigma_{axial\,max} = \frac{M_{axial\,max} c}{I} = \frac{\frac{F_{axial} L}{8} \frac{h}{2}}{\frac{bh^3}{12}} = \frac{3Eh}{2L^2} \delta_{axial} \tag{19}$$

3.5 Fatigue analysis

The modified Basquin equation is used to determine the life cycle till failure; the life cycle is calculated as below (Spotts et al., 2004)

$$N = \left(\frac{\sigma_R}{A} \right)^{\frac{1}{B}} \tag{20}$$

where σ_R is the completely equivalent reverse stress, which can be determined by A and B as following

$$\sigma_R = \frac{K_f \sigma_r \sigma_u}{\sigma_u - \sigma_{avg}} \tag{21}$$

$$A = \frac{\sigma_e}{10^{6B}} \tag{22}$$

$$B = \frac{\log(\sigma_e) - \log(0.9\sigma_u)}{3} \tag{23}$$

where K_f is the fatigue stress concentration factor, σ_r the range stress, σ_u the ultimate strength, σ_{avg} the average stress, σ_e the endurance limit.

4 Preliminary results and discussion

The material properties of the spring steel are: Young's modulus E of 210 GPa; the Poisson's ratio, ν, of 0.3; the density, ρ, of 7.85×10^{-3} g mm^{-3}; the ultimate strength, σ_u, of 1274 MPa; the endurance limit, σ_e, of 700 MPa. The fatigue stress concentration factor K_f is 1.4.

All the dimensions of the FTS are determined by above detailed analysis. The dimensions of the CM are shown in Table 1. The mass of the rigid part m_s is approximately 104.9074 g. The first natural frequency is 1578 Hz. The safety factor S_f is assumed 1.05.

The applied forces are assumed: cutting force F_c of 10 N; feed force F_f of 10 N; the preload axial force of 20.635 N; the maximum axial force of 206.346 N.

4.1 Design analysis results

Some critical parameters of the FTS are obtained; the axial stiffness K_{axial} is 10.3173 N μm^{-1}; both the horizontal stiffness $K_{horizontal}$ and the vertical stiffness $K_{vertical}$ are 0.714 N nm^{-1}.

The horizontal force applied to the front set of beams F_{h1} and that in the rear set of beams F_{h2} are 17.69 N and 7.69 N, respectively. The vertical force applied to the front set of beams F_{v1} and that in the rear set of beams F_{v2} are 17.69 N and 7.69 N, respectively. The horizontal displacements of the end of front set of beams δ_{h1} and that in the rear set of beams δ_{h2} are 24.78 nm and 10.78 nm, respectively. The vertical displacements of the end of front set of beams δ_{v1} and that in the rear set of beams δ_{v2} are 24.78 nm and 10.78 nm, respectively.

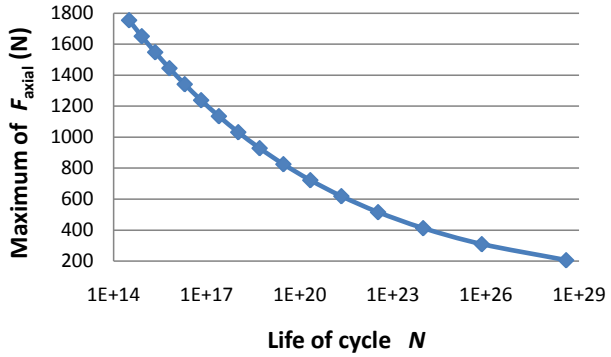

Figure 5. Relationship between the maximum axial force and the life cycle.

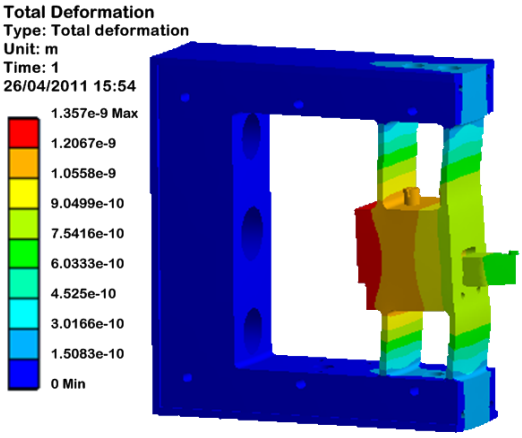

Figure 6. Deformation of the CM structure only subjected to gravity.

The relationship between the maximum axial force and the life cycle N is shown in Fig. 5. It clearly shows the life cycle is more than 10^{28} when the maximum axial force is 206.346 N. Therefore, fatigue failure will not occur.

4.2 FEA results

In order to verify the results of the design analysis method, FEM is used to doing static analysis of the CM structure including the cutting tool and its locking bolts.

The first static analysis was to investigate the influence of gravity on the tool tip and gave a value of 1.3 nm as shown in Fig. 6.

The first reason for finding the value for static analysis is to evaluate the displacement from gravitational force error when the machine is in static conditions. The second reason was finding the weakest point of the FTS structure which will make the greatest effect during machining in term of further modification and model updating. From that point of view, the modal analysis was performed under the same conditions. Figure 7 shows the modes shape of the desktop machine including 1st mode 1634 Hz (actuation in Z-axis, i.e., axial direction), 2nd mode 6947 Hz (twisting, left-right in Y-axis), 3rd mode, 8792 Hz (twisting and bending) and 4th mode 12 305 Hz (twisting in X-axis).

Figure 8 shows the shear stress analysis in X-, Y- and Z-directions. Both in the directions of X and Y 10 N are applied to investigate the shear area. In the Z-direction, the applied force is 200 N for investigating the stiffness of the CM. It clearly shows in Fig. 8 that the maximum shear stress occurs around the hinges where the beams connected with the rigid part or the base. The red colour presents where the maximum shear stress occurs.

The displacement in Z-direction when force is applied from 0 to 200 N, increased by 10 N, is analyzed. The relationship between the displacement and the force in the Z direction shows in Fig. 9. It can be observed that the relationship between them is in the linear manner. The gradient of the line; the axial stiffness of the CM in the axial direction is 11.979 N μm^{-1}; the correlation coefficient is 1.0; the Y-intercept is −0.0248 N.

4.3 Discussion

1. The first natural frequency of the CM analyzed by FEA is close to the detailed analysis. The FTS can work at no more than 1400 Hz which is less than 10 % of the first natural frequency 1634 Hz.

2. Both the vertical and horizontal stiffness are greater than the axial stiffness and their displacements are very small when applied cutting force and feed force. This kind of design of the CM assures the 1DOF motion of the tool tip and the manufacturing accuracy.

3. The smaller the length of the tool tip protruding from the rigid part of the CM is, the smaller the displacement of the rigid part in horizontal and vertical directions becomes. The high rigidity of the tool is necessary.

4. Fatigue should not occur in the FTS during the analysis.

5 Conclusions

A comprehensive and robust design method of compliant fast tool servo, which has a 1DOF translational motion, for precision engineering is presented. The stiffness in three directions and the first natural frequency of the CM can be predetermined. The reaction forces and maximum deformation analysis of the CM can be calculated. The results of FEA are matching to that of the design requirements. The fatigue of the CM is predicted and it should work without failure.

The author would like to report the experimental cutting trial results by using the fast tool servo in alignment with the FEA-based simulation and analysis as an extension in the future.

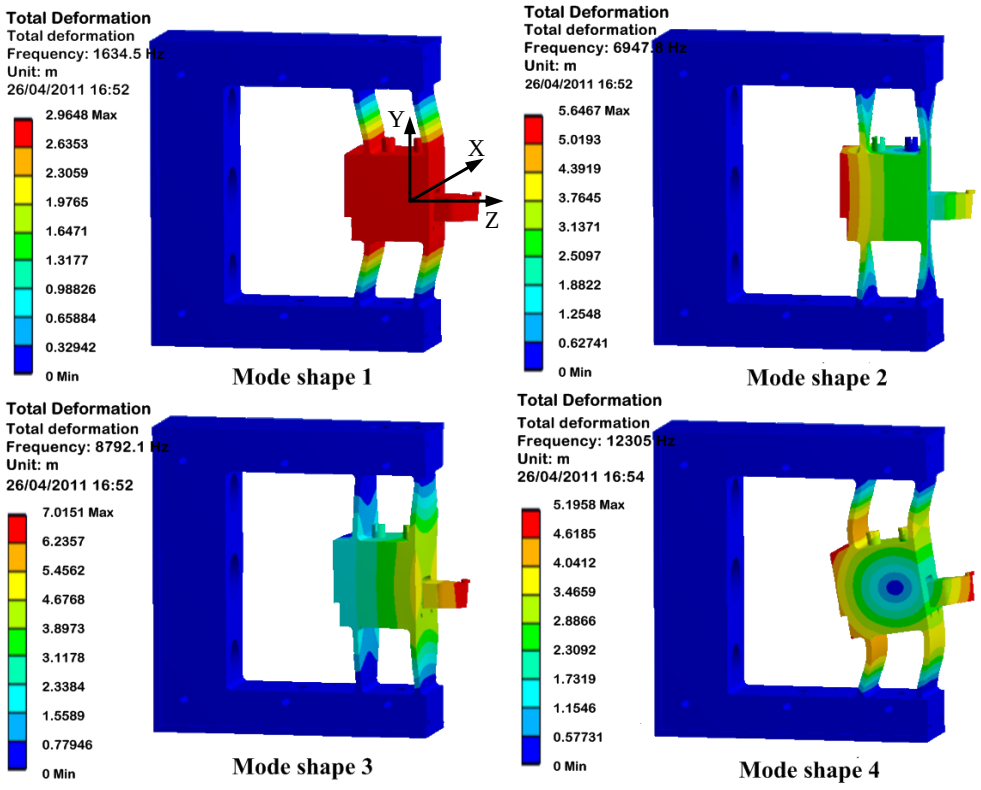

Figure 7. The first four natural frequencies and mode shapes.

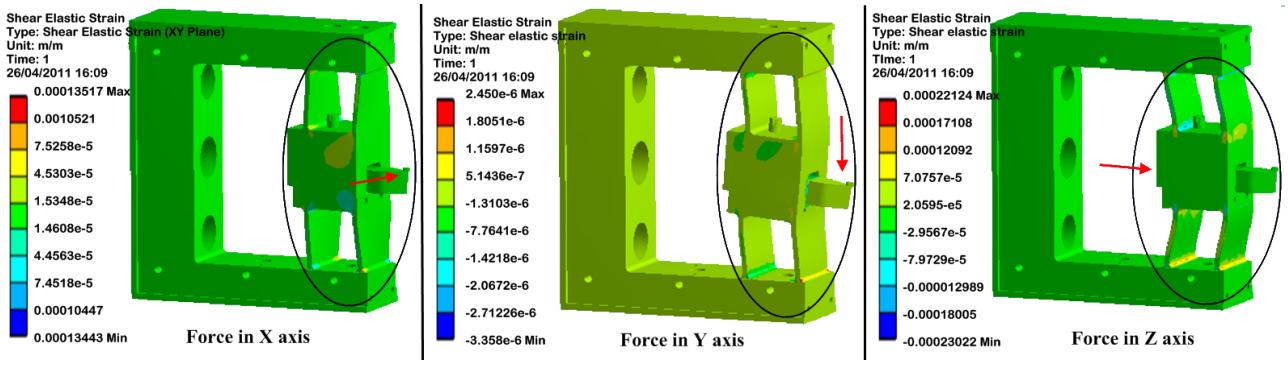

Figure 8. The shear stain and stress area in X-, Y- and Z-direction applied force.

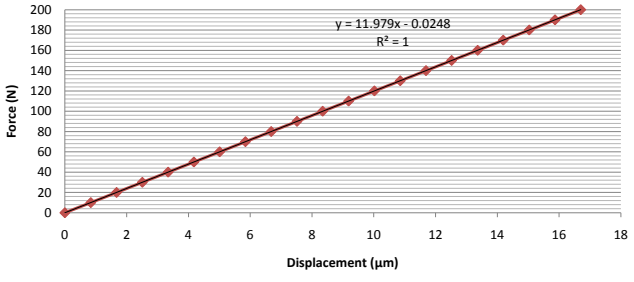

Figure 9. Stiffness experiment in Z-axis.

Acknowledgements. The authors would like to thank Paul Yates and Chao Wang at Brunel University for helpful discussions and the partial support of The National High-tech R&D Program (863 Program, SQ200802LS1479459) for funding the visiting project at Brunel University.

Edited by: N. Tolou
Reviewed by: three anonymous referees

References

Cuttino, J. F., Miller, A. C., and Schinstock, D. E.: Performance optimization of a fast tool servo for single-point diamond turning machines, IEEE-ASME T. Mech., 4, 169–179, 1999.

Gan, S. W., Lim, H. S., Rahman, M., and Watt, F.: A fine tool servo for global position error compensation for a miniature ultra-precision lathe, Int. J. Mach. Tool. Manu., 47, 1302–1310, 2007.

Howell, L. L.: Compliant Mechanisms, John Wiley & Sons, Inc., New York, USA, 2001.

Huo, D. and Cheng, K.: A dynamics-driven approach to the design of precision machine tools for micro-manufacturing and its implementation perspectives, in: Proceedings of ImechE Part B: Journal of Engineering Manufacture, 222, 1–13, 2008.

Kim, H. S. and Kim, E. J.: Feed-forward control of fast tool servo for real-time correction of spindle error in diamond turning of flat surfaces, Int. J. Mach. Tool. Manu., 43, 1177–1183, 2003.

Kim, H. S., Kim, E. J., and Song, B. S.: Diamond turning of large off-axis aspheric mirrors using a fast tool servo with on-machine measurement, J. Mater. Process. Tech., 146, 349–355, 2004.

Kim, H. S., Lee, K. I., Lee, K. M., and Bang, Y. B.: Fabrication of free-form surfaces using a long-stroke fast tool servo and corrective figuring with on-machine measurement, Int. J. Mach. Tool. Manu., 49, 991–997, 2009.

Kouno, E.: A fast response piezoelectric actuator for servo correction of systematic errors in precision machining, Annals of the CIRP, 33, 369–372, 1984.

Li, S. Z., Yu, J. J., Pei, X., Su, H. J., Hopkins, J. B., and Culpepper, M. L.: Type synthesis principle and practice of flexure systems in the framework of screw theory Part III: numerations and type synthesis of flexure mechanisms, in: Proceeding of the ASME 2010 international design engineering technical conferences & computers and information in engineering conference IDETC/CIE 2010, Montreal, Quebec, Canada, 15–18 August 2010, DETC2010-28963, 2010.

Noh, Y. J., Nagashima, M., Arai, Y., and Gao, W.: Fast positioning of cutting tool by a voice coil actuator for micro-lens fabrication, International Journal of Automation Technology, 3, 257–262, 2009.

Spotts, M. F., Shoup, T. E., and Hornberger, L. E.: Design of Machine Elements, 8th Edn., Pearson Prentice Hall, New Jersey, 2004.

Tian, Y., Shirinzadeh, B., and Zhang, D.: A flexure-based mechanism and control methodology for ultra-precision turning operation, Precis. Eng., 33, 160–166, 2009.

Yu, J. J., Li, S. Z., Pei, X., Su, H. J., Hopkins, J. B., and Culpepper, M. L.: Type synthesis principle and practice of flexure systems in the framework of screw theory Part I: general methodology, in: Proceeding of the ASME 2010 international design engineering technical conferences & computers and information in engineering conference IDETC/CIE 2010, Montreal, Quebec, Canada, 15–18 August 2010, DETC2010-28783, 2010a.

Yu, J. J., Pei, X., Li, S. Z., Su, H. J., Hopkins, J. B., Culpepper, M. L.: Type synthesis principle and practice of flexure systems in the framework of screw theory Part II: numerations and synthesis of complex flexible joints, in: Proceeding of the ASME 2010 international design engineering technical conferences & computers and information in engineering conference IDETC/CIE 2010, Montreal, Quebec, Canada, 15–18 August 2010, DETC2010-28794, 2010b.